INTERNATIONAL JOURNAL OF INTEGRATED ENGINEERING
ISSN: 2229-838X e-ISSN: 2600-7916

IJIE

Vol. 17 No. 8 (2025) 148-158
https://publisher.uthm.edu.my/ojs/index.php/ijie

Development of a Tiltrotor Propulsion System for Hybrid VTOL Fixed-Wing Drones

Mohd Fadhli Zulkafli[1]*, Lau Wei Le[1], Bong Zhan Yong[1], Ahmad Hamdan Ariffin[1,2], Syafiqah Nur Azrie Safri[1,2], Mohd Fauzi Yaakub[1,2]

[1] *Research Center for Unmanned Vehicle, Faculty of Mechanical and Manufacturing Engineering, Universiti Tun Hussein Onn Malaysia, Parit Raja, 86400 Batu Pahat, Johor, MALAYSIA*
[2] *Department of Aeronautical Engineering, Faculty of Mechanical and Manufacturing Engineering, Universiti Tun Hussein Onn Malaysia, Parit Raja, 86400 Batu Pahat, Johor, MALAYSIA*

*Corresponding Author: fadhli@uthm.edu.my
DOI: https://doi.org/10.30880/ijie.2025.17.08.014

Article Info

Received: 1 June 2025
Accepted: 20 November 2025
Available online: 31 December 2025

Keywords

Drone, hybrid fixed-wing drone, VTOL, tilt rotor, PolyTerra PLA

Abstract

Hybrid Unmanned Aerial Vehicles (UAVs) integrate features from both fixed-wing and multirotor UAVs. The fixed wings efficiently distribute aerodynamic loads while combining aerodynamic properties with the multirotor configuration. A tiltrotor mechanism is necessary to facilitate the transition between hover and forward flight modes. This research focuses on developing a comprehensive tiltrotor propulsion system for a fixed-wing aircraft. Two methodologies were employed: software simulation and experimental testing. A restricted flight test was conducted using a test rig to observe the drone's behaviour at various throttle levels, revealing that each motor produced 2.12 kg of thrust, resulting in a total thrust of 6.12 kg. The drone successfully lifts off at its maximum take-off weight of 3.1 kg. Five potential materials for the components supporting the front and rear motors were tested through simulations, with Polymaker's PolyTerra PLA, a modified polylactic acid material, proving to be the best option. It demonstrated maximum equivalent von Mises stress values of 4.0122 MPa for the front motor supports and 2.8205 MPa for the rear motor supports, along with minimal deformations of less than 0.01 mm. Therefore, the results demonstrate that Polymaker's PolyTerra PLA is an optimal material for the support components of the front and rear rotors, ensuring structural reliability and suitability for hybrid vertical take-off and landing (VTOL) fixed-wing drones, as evidenced by its exceptional performance under simulated and experimental conditions.

1. Introduction

Unmanned Aerial Vehicles (UAVs) have grown across numerous industries as military [1–4], agriculture [5–7], surveillance [8–10], and others. Fixed-wing aircraft and helicopters with rotary motors are the two primary forms of UAVs. Fixed-wing aircraft are powered by turbine jet engines or propellers to move forward. They are widely used for both military and commercial applications since they can travel farther and produce less noise than traditional aircraft. But normal flight is dependent on the conditions of take-off, and they are unable to hover around easily [11]. Rotating motor UAVs can fly in a stationary hover and have greater precision in smaller spaces; however, because they typically have four or more motors operating in them, their battery life is shorter. Despite this, they can perform take-offs and landings without requiring large terrain [12]. To overcome these limitations, hybrid vertical take-off and landing (VTOL) fixed-wing drones have been developed. These drones are designed

to seamlessly transition between vertical take-off and landing to forward flight, combining the best features of both aircraft types. It resulted in the creation of tilt-rotor, hybrid, and fixed-wing VTOL aircraft [13]. The fixed-wing/quadcopter hybrid's efficiency, range, and flying duration can all be increased by its ability to glide during a cruise with a minimal thrust-to-weight ratio [14].

Tilt rotors allow the hybrid UAVs to convert from one flight mode to another, enhance their manoeuvrability, and permit the aircraft to be configured to meet mission requirements [15]. Tilt rotor technology has been the subject of extensive research and development in the field of unmanned aerial vehicles. Previous studies have focused on the aerodynamic efficiency and control mechanisms of tilt rotor systems, aiming to enhance the overall performance and versatility of hybrid UAVs with fixed-wing capabilities [16]. Additionally, researchers have explored the integration of tilt-rotor technology with advanced flight control systems to further optimise the operational capabilities of these hybrid aircraft [17]. These efforts have contributed to the advancement of tilt-rotor technology and its potential for revolutionising the capabilities of hybrid UAVs in a wide range of applications. The most alluring aspect of hybrid aerial vehicles is their ability to achieve significantly higher cruising speeds than conventional rotorcraft when in aircraft mode and to hover like a helicopter, all because of the adjustable rotor tilt angle. Therefore, one of the best concepts for fusing the advantages of rotorcraft and fixed wings in a range of uses is the tiltrotor aircraft [18].

This study aims to develop a tiltrotor hybrid drone that can take off and land vertically (VTOL) and have the aerodynamic stability of a fixed-wing drone. This will be achieved by designing a tiltrotor propulsion system on a fixed-wing model. The tiltrotor system will allow the drone to transition from a multirotor drone to a fixed-wing drone and efficiently fly long distances using an unmanned remote-control system [19]. In this design, the cruise motor is used for hovering and forward flight, although it is supplemented with a separate powered lift system. This keeps the efficiency loss of the cruise propulsion system within allowable limits while minimising the large weight and volume increase for a customised propulsion system. Five different materials will be proposed as suitable materials for the drone motor. These materials will undergo simulations to test their performance to ensure the best material for this newly developed drone.

2. Methodology

2.1 Drone Prototype

The tiltrotor hybrid drone is equipped with three motors. Two of these motors, positioned in front of the left and right sides of the wing, are fitted with tilting mechanisms. The third motor is fixed and located at the rear of the drone, as illustrated in Fig. 1. The tilting mechanism changes the flight mode from hover to cruise and vice versa. The airframe body uses the Mini Skywalker model [20], which is made from polystyrene foam, as shown in Fig. 2, while the wing is supported by a spar made from carbon fibre. The motor used is a 700 - 400KV Tarot 650 KV brushless DC motor paired with a propeller size 14-inch diameter carbon fibre propeller fitted on the tilting and fixed rotor system. In addition, the maximum lift-to-drag ratio for this drone during cruising is 12.

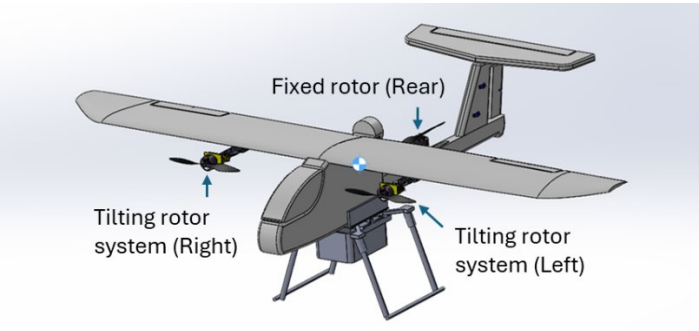

Fig. 1 *CAD view of tricopter VTOL drone prototype with tilting rotor system*

Fig. 2 *Fully assembled VTOL drone prototype*

Int. Journal of Integrated Engineering Vol. 17 No. 8 (2025) p. 148-158

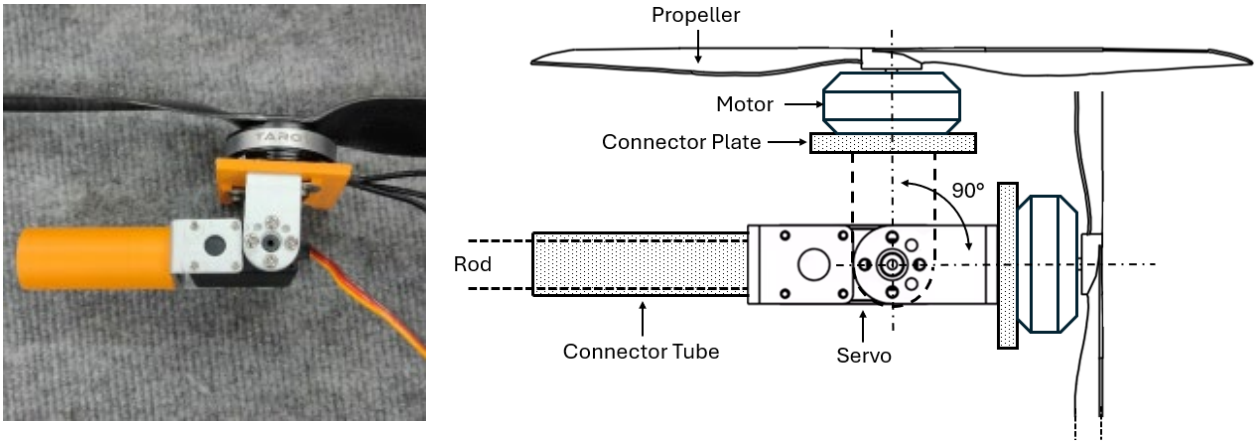

(a) **(b)**

Fig. 3 *(a) Actual; and (b) Schematic diagram of tilting rotor system design*

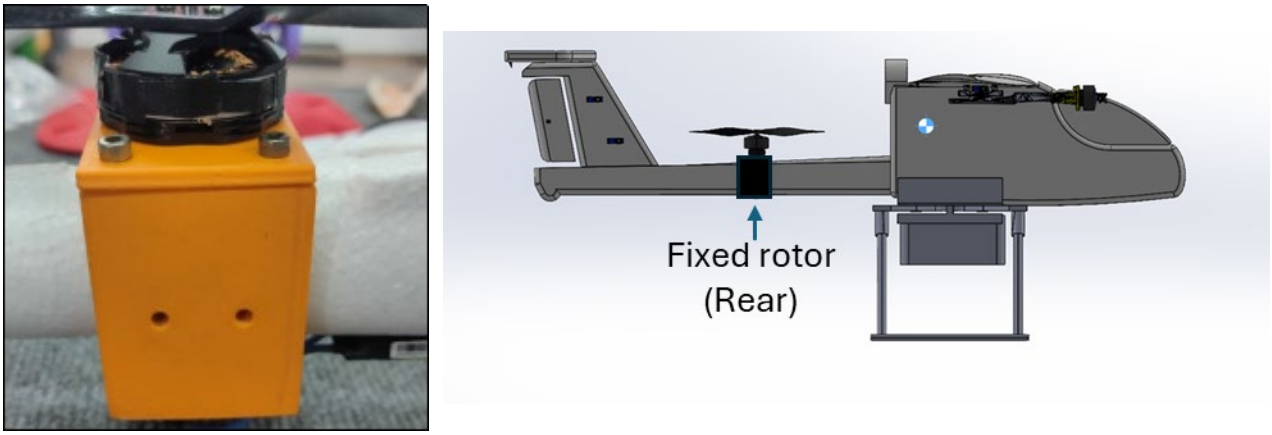

(a) **(b)**

Fig. 4 *Rear rotor attached to the (a) actual connector housing; and (b) CAD design of the drone tail*

A tilt mechanism design, shown in Fig. 3, enables the front motor to tilt 90 degrees during the changing flight mode from the hover to cruise or forward flight, illustrating the assembly of the rear motor to the drone's body. The motor is attached to a connector housing, which is then mounted to the drone's body. The housing is composed of two connector parts and two connector plates. Four M3 screws are used to secure each connector part and the two connector plates. Additionally, both sides of the connector parts are fastened with two M4 screws to secure them firmly to the drone.

The total weight of all the prototypes, including the payload, adds up to 3 kg as shown in Table 1. This weight is an overestimation, as it is preferable to have excess power rather than underestimating it [21]. As a general rule, the total thrust produced by all motors should be at least double the drone's total weight [22]. A 2:1 or 3:1 thrust-to-weight ratio is just nice for a drone to have better control and extra room for payload in the future [23]. Therefore, for a 2:1 thrust-to-weight ratio, this drone's propulsion system must generate more than 6 kg of thrust.

Table 1 *Drone weight specification*

Items	Weight (kg)
Airframe	0.25
Battery	0.22
Propulsion system and servo	1.53
Total Drone Weight	2.00
Maximum Payload Weight	1.00
Total Target Flying Weight	3.00

2.2 Restricted Flight Test on a Test Rig

Fig. 5 illustrates the setup for testing the drone's propulsion system using a test rig. In this arrangement, the drone is mounted on the rig to allow for both vertical and rotational movement. The vertical movement simulates the drone's ability to ascend and descend, allowing for thrust measurement relative to its weight. In contrast, the rotational movement tests yaw control and how the propulsion system manages directional changes and flight stability. These movements are crucial for simulating flight conditions and evaluating the drone's control and propulsion capabilities in a controlled environment. The data gathering system is attached to the test rig, which captures critical information during the test, such as thrust, torque, and power consumption. This data is essential for analysing the performance of the propulsion system under different conditions.

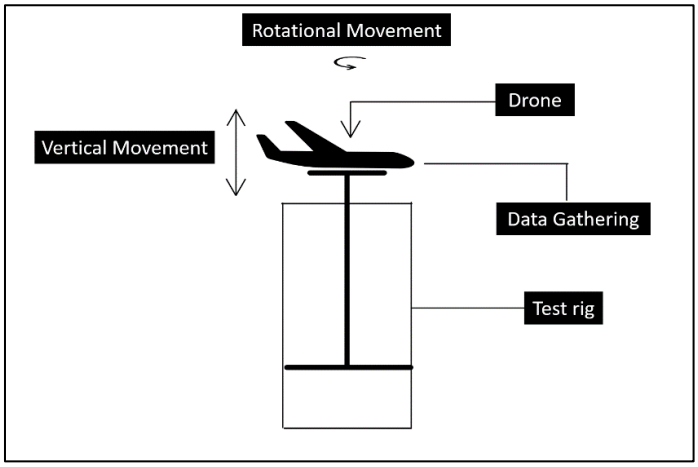

Fig. 5 *Schematic diagram of drone with test rig*

2.3 Structural Analysis Setup

The suitability of PolyTerra PLA as a material for 3D printing the connector plate for the tilting rotor and the connector housing for the fixed rotor systems was evaluated using the Static Structural Analysis module in Ansys Mechanical software. The CAD models for the motor support of the tilting mechanism and the connector housing were created using SolidWorks, with designs based on the actual dimensions of the existing drone. These models were then imported into Ansys Workbench for the structural analysis. Several parameters were adjusted to optimise the results. First, fixed supports were applied at the front and rear of the drone to prevent any displacement or movement. The drone's maximum thrust was set at 2.12 kg (21.2 N), used as the force parameter with the assumption of no wind resistance or drag. Finally, a downward force was applied to the contact surface of the connector plate, and the thrust was evenly distributed across the three screws and the surface.

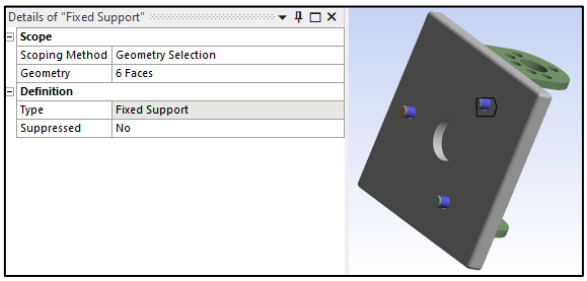

Fig. 6 *Support for front drone*

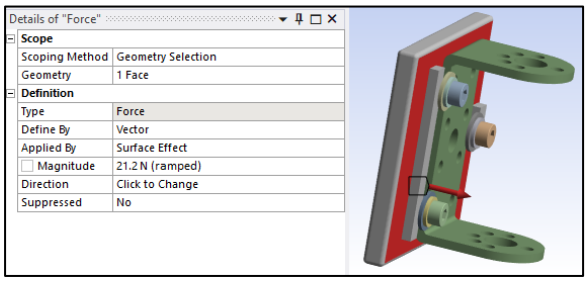

Fig. 7 *Force for front drone*

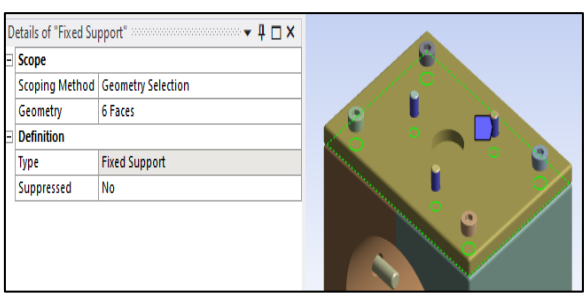

Fig. 8 *Fixed support for rear drone*

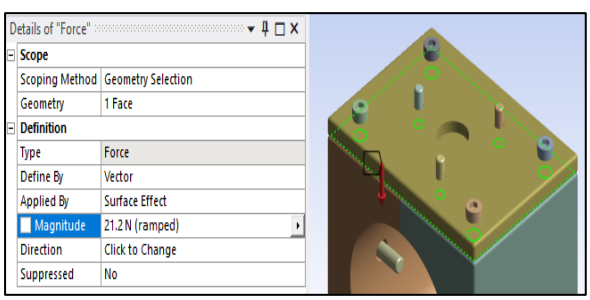

Fig. 9 *Force applied on the connector housing*

Int. Journal of Integrated Engineering Vol. 17 No. 8 (2025) p. 148-158

Fig. 6 shows the CAD design of the connector plate for the front motor, as imported into Ansys Mechanical, and Fig. 7 illustrates the forces acting on that support, indicated by the red-highlighted geometry face. Fig. 8 presents the CAD design of the connector housing for the rear motor, while Fig. 9 depicts the force applied to the surface of the connector housing, shown as a hidden green dotted surface.

Five materials were used in the simulation results: structural steel, PolyTerra PLA, aluminum alloy 6061, carbon steel 1020, and low alloy steel 4140, as shown in Table 2. Structural steel was the default material for the simulation, while PolyTerra PLA was the material used for 3D printing connector plates and connector housing. The other three materials serve as alternatives in case structural failure occurs with PolyTerra PLA. These materials can be added from the Engineering Data Sources in Ansys Workbench. Tensile strength is required for the safety factor in the simulation, making it essential to obtain a tensile strength value of 20.9 MPa.

Table 2 *List of materials used for the simulation*

Material	Description
Aluminium alloy, wrought, 6061, T6	Data compiled by Ansys Granta, incorporating various sources, including JAHM and Mag Web
Carbon steel, 1020, annealed	Data compiled by Ansys Granta, incorporating various sources, including JAHM and Mag Web
Low alloy steel, 4140, normalized.	Data compiled by Ansys Granta, incorporating various sources, including JAHM and Mag Web
Polyterra PLA	Young's Modulus: 1882 +/- 141MPa
	Tensile Strength: 20.9 +/- 2.0MPa
	Bending Strength: 39.6 +/- 1.1MPa
	Charpy Impact Strength: 5.7 +/- 0.4Kj/m^2
Structural Steel	Fatigue Data at zero mean stress comes from 1998 AMSE BPV Code, Section 8, Div 2, Table 5-110.1

3. Results and discussion

3.1 Performance of the Propulsion System

Using the mission planner, the arming throttle can be determined by testing the motor with different throttle inputs, setting the throttle percentage, and observing the motor's rotation. If the motor rotates, it indicates that it is armed, establishing the minimum throttle required to arm the motor. As shown in Table 3, the results indicate that all motors are armed and spinning at 25% throttle. Therefore, it can be concluded that the arming throttle should be set above 25%.

A tachometer was used to measure the motor's RPM, which varies according to the throttle input. Table 4 shows that at 30% throttle, all motors are armed. The rear motor achieves the desired speed with a lower input because it is the only motor positioned at the rear of the aircraft. Consequently, the proportion of input to output is greater compared to the two front motors. The results also indicate that a small throttle input is sufficient to initiate motor rotation.

Table 3 *Throttle and motor behaviour*

Throttle (%)	Motor		
	Left	Right	Rear
20	Unarmed	Armed	Unarmed
21	Unarmed	Armed	Unarmed
22	Unarmed	Armed	Unarmed
23	Unarmed	Armed	Unarmed
24	Armed	Armed	Unarmed
25	Armed	Armed	Armed

Table 4 *Throttle and RPM of motor*

Throttle (%)	RPM of Motor		
	Left	Right	Rear
20	0	1166	0
30	1701	1980	1592
40	2816	2900	2500
50	3350	3660	3226
60	4560	5045	4410

Table 5 *Throttle and motor thrust*

Throttle (%)	Average Thrust (kg)
30	0.85
40	1.03
50	1.21
60	1.39
70	1.58
80	1.77
90	1.95
100	2.12

The minimum thrust for this drone is determined by calculating the thrust required during steady cruising flight. The thrust required during level cruise can be determined by the balance of aerodynamic forces, where thrust (T) equals drag (D) and lift (L) equals weight (W). For a drone with a maximum take-off weight of 3.1 kg and a lift-to-drag (L/D) ratio of 12, the drag force can be calculated using the relationship $D = W(L/D)$, which results in a required thrust of approximately 0.25 kg. Since the drone has a tri-motor configuration, the thrust contribution per motor would be approximately 0.083 kg. However, in practical flight conditions, a higher thrust capacity will be necessary to compensate for factors such as wind resistance, turbulence, and additional flight control adjustments.

The thrust generated by the motor is measured using an in-house-built thrust test rig. The motor is mounted on the test rig and tested at different throttle levels. As shown in Table 5, the maximum total thrust the drone can generate is 2.12 kg per motor, resulting in a total of 6.36 kg. This gives a thrust-to-weight ratio of 6.36 kg to 3.1 kg, which equals 2.05. Therefore, this thrust is sufficient to provide lift during take-off and landing, as the maximum thrust is more than double the drone's weight. The maximum thrust value, determined to provide a base for material strength analysis using Ansys Mechanical software, is crucial for selecting a material for the connector plate of the tilting rotor and the connector housing of the fixed rotor systems. The material must be lightweight and low-cost while being strong enough to withstand the load from the maximum thrust.

3.2 Tilt Rotor Mechanism

Fig. 10, Fig. 11, and Fig. 12 show the tiltrotor system in hover mode, transitioning from hover to forward flight, and forward flight mode, respectively. In Fig. 10, the drone is in hover mode, where the tiltrotor system maintains a vertical orientation for stable hovering, balancing the thrust from the front and rear motors. In Fig. 11, the transition stage is depicted, where the front motors are gradually tilting forward to shift the drone from hovering to forward flight. This transition is smooth and stable, allowing the drone to adjust its flight mode efficiently.

Fig. 10 *Tilt rotor system in hover mode*

Int. Journal of Integrated Engineering Vol. 17 No. 8 (2025) p. 148-158

Fig. 11 *Tilt rotor system during transition*

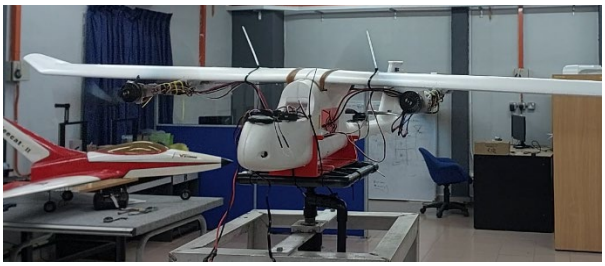

Fig. 12 *Tilt rotor system in forward flight mode*

Fig. 12 shows the drone in full forward flight mode, with the rotors achieving horizontal orientation for forward propulsion. The results indicate that the tiltrotor mechanism achieves a stable and smooth transition between hover and forward flight, validating the mechanical design and control strategy. The servo system effectively counters gyroscopic moments generated by the large, fast-spinning rotors, a critical requirement noted in [24]. This ensures operational smoothness and allows for potential upgrades with more powerful motors to enhance payload capacity.

The restricted flight test demonstrated that the drone successfully lifted off with a throttle input of approximately 60% to 70%. The drone, weighing 3.1 kg and equipped with three rotors, generated sufficient thrust for a stable take-off within this throttle range. The average thrust per rotor was measured at 1.39 kg at 60% throttle and 1.58 kg at 70% throttle input, while the maximum thrust per rotor was 2.12 kg, as shown in Table 5. Collectively, the thrust provided adequate lift for a stable take-off. Based on the guideline that the total thrust should be at least double the drone's total weight for efficient VTOL performance [22], the combined thrust output meets this requirement, indicating the tiltrotor system's capability to fulfill the thrust demands for this hybrid VTOL drone.

3.3 Material Analysis

The results for the total deformation of the rear and front motors, shown in Fig. 13 - Fig. 20, are summarised in Tables 6 and 7 for data analysis. Table 6 presents the simulation results for the front motor, including maximum total deformation, maximum directional deformation along the Z, Y, and X axes, and maximum equivalent stress for PolyTerra PLA, Aluminum Alloy 6061, Carbon Steel 1020, and Low Alloy Steel 4140. Consistent with the data [25], Carbon Steel 1020 exhibited the least deformation across all axes and the highest equivalent stress, making it suitable for load-bearing applications. In addition, Table 7 presents the simulation results for the rear motor under the same conditions. Again, Carbon Steel 1020 demonstrated the least deformation and the highest equivalent stress among the materials.

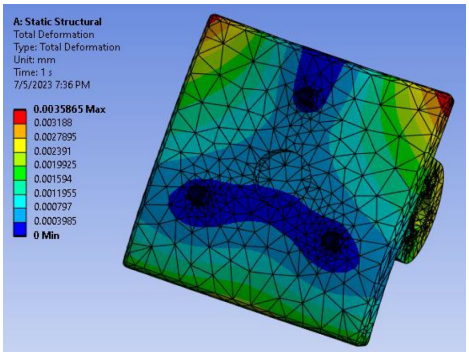

Fig. 13 *Total deformation of the front motor's connector plate (PolyTerra PLA)*

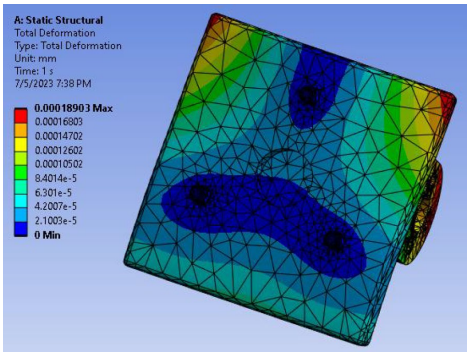

Fig. 14 *Total deformation of the front motor's connector plate (Aluminium alloy 6061)*

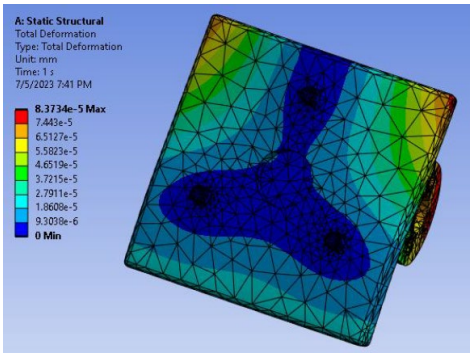

Fig. 15 *Total deformation of the front motor's connector plate (Carbon steel 1020)*

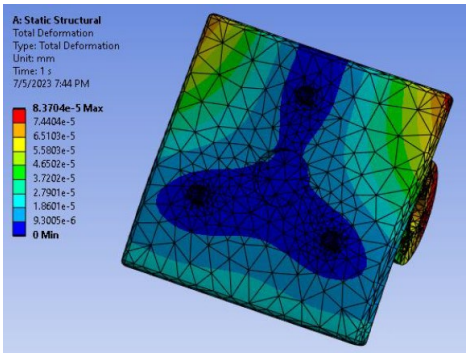

Fig. 16 *Total deformation of front motor's connector plate (Low alloy steel 4140)*

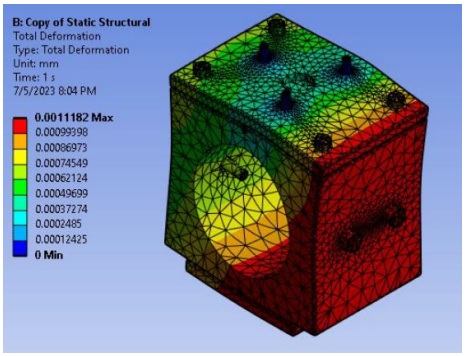

Fig. 17 *Total deformation of the rear motor's connector housing (PolyTerra PLA)*

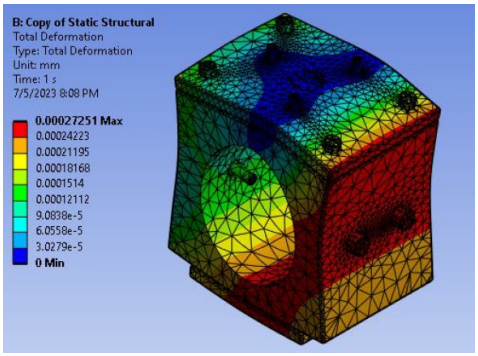

Fig. 18 *Total deformation of the rear motor's connector housing (Aluminium alloy 6061)*

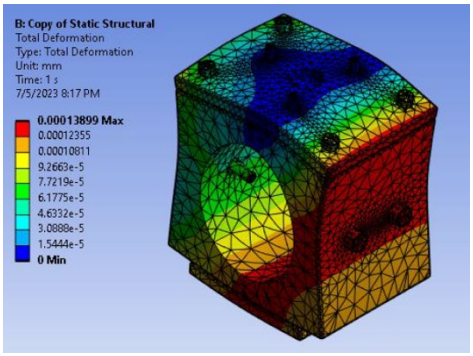

Fig. 19 *Total deformation of the rear motor's connector housing (Carbon steel 1020)*

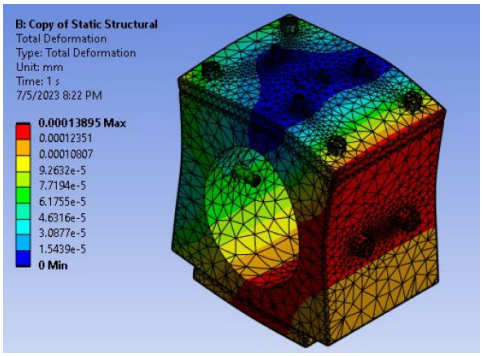

Fig. 20 *Total deformation of the rear motor's connector housing (Low alloy steel 4140)*

Table 6 *Performance of the front motor*

	PolyTerra PLA	Aluminum Alloy 6061	Carbon Steel 1020	Low Alloy Steel 4140
Max. Total Deformation (mm)	$3.5865\ e^{-3}$	$1.8903\ e^{-4}$	$8.3734\ e^{-5}$	$8.3704\ e^{-5}$
Max. Directional Deformation Z-axis (mm)	$5.0444\ e^{-5}$	$2.8398\ e^{-6}$	$1.4255\ e^{-6}$	$1.4251\ e^{-6}$
Max. Directional Deformation Y-axis (mm)	$3.9784\ e^{-4}$	$1.3395\ e^{-5}$	$5.2701\ e^{-6}$	$5.2682\ e^{-6}$
Max. Directional Deformation X-axis (mm)	$1.3326\ e^{-3}$	$1.0489\ e^{-4}$	$4.8939\ e^{-5}$	$4.8922\ e^{-5}$
Max. Equivalent Stress (von-Mises) (MPa)	4.0122	1.5721	1.7040	1.7040

Int. Journal of Integrated Engineering Vol. 17 No. 8 (2025) p. 148-158

Table 7 *Performance of the rear motor*

	PolyTerra PLA	Aluminum Alloy 6061	Carbon Steel 1020	Low Alloy Steel 4140
Max. Total Deformation (mm)	1.1182 e^{-3}	2.7251 e^{-4}	1.3889 e^{-4}	1.3895 e^{-4}
Max. Directional Deformation Z-axis (mm)	1.1491 e^{-4}	1.9825 e^{-5}	1.1285 e^{-5}	1.1273 e^{-5}
Max. Directional Deformation Y-axis (mm)	2.0318 e^{-5}	4.8215 e^{-7}	3.2108 e^{-7}	3.2099 e^{-7}
Max. Directional Deformation X-axis (mm)	2.2333 e^{-5}	6.0237 e^{-5}	3.3560 e^{-5}	3.3550 e^{-5}
Max. Equivalent Stress (von-Mises) (MPa)	2.8205	1.9373	1.5519	1.5520

PolyTerra PLA exhibited higher deformation and equivalent stress values in both motor configurations compared to the metallic counterparts. However, the material remained structurally adequate, with a minimum safety factor greater than one for both the front motor connector plates and the rear motor connector housing. The equivalent von Mises stress values were 4.0122 MPa for the front motor part and 2.8205 MPa for the rear motor part, both well below the PolyTerra PLA yield strength of 20.9 MPa (Table 2), indicating no risk of material failure under the tested conditions. This suggests PolyTerra PLA can be safely used when the maximum thrust per rotor is 2.12 kg.

From a comparative perspective, minimal differences were observed between Carbon Steel 1020 and Low Alloy Steel 4140 in terms of total deformation, directional deformations along the Z, Y, and X axes, and maximum equivalent stress. The Young's modulus of Carbon Steel 1020 (2.125 MPa) closely matches that of Low Alloy Steel 4140 (2.125 MPa), differing by only 1 kPa. However, Carbon Steel 1020 demonstrated significantly higher tensile strength (1015 MPa) compared to Low Alloy Steel 4140 (393 MPa). As tensile strength is a critical factor in determining material yielding under mechanical stress [26], Carbon Steel 1020's superior tensile strength highlights its suitability for load-bearing components, while the higher ductility of Low Alloy Steel 4140 provides better resistance to sudden impact loads [27], making it suitable for applications requiring toughness.

4. Conclusions

The development and evaluation of the tiltrotor propulsion system for a hybrid VTOL fixed-wing drone presented in this study successfully demonstrated both structural reliability and aerodynamic efficiency. The tiltrotor system effectively facilitated smooth transitions between hover and forward flight modes, as confirmed through experimental testing on a restricted flight test rig. The propulsion system was capable of generating a maximum thrust of 6.12 kg, ensuring sufficient lift for stable take-off with a maximum take-off weight of 3.1 kg, meeting the recommended thrust-to-weight ratio of 2:1 for efficient VTOL performance.

Material analysis confirmed that PolyTerra PLA, among the tested materials (Aluminum Alloy 6061, Carbon Steel 1020, and Low Alloy Steel 4140), exhibited adequate structural performance for the motor support components. With a maximum von Mises stress of 4.0122 MPa for the front motor and 2.8205 MPa for the rear motor, both well below the material's yield strength of 20.9 MPa, PolyTerra PLA demonstrated sufficient mechanical strength with a safety factor exceeding the critical threshold. Minimal deformations observed further support its viability for lightweight UAV structures. Overall, the findings validate the structural integrity and operational effectiveness of the tiltrotor propulsion system. The combination of experimental testing and simulation analysis confirms the suitability of PolyTerra PLA for supporting the front and rear rotors in hybrid VTOL fixed-wing drones.

Acknowledgement

This research was supported by Universiti Tun Hussein Onn Malaysia (UTHM) through Tier 1 (voteQ496) and Tier 1 (voteQ498). This research was also supported by the Ministry of Higher Education (MOHE) through the Fundamental Research Grant Scheme (FRGS/1/2020/TK02/UTHM/02/3). The authors would also wish to express sincere gratitude and gratefully acknowledge the support received from the Faculty of Mechanical and Manufacturing Engineering, UTHM.

Conflict of Interest

The authors declare that there is no conflict of interest regarding the publication of the paper.

Author Contribution

The authors confirm contribution to the paper as follows: ***study conception and design:*** *Mohd Fadhli Zulkafli, Ahmad Hamdan Ariffin;* ***data collection:*** *Lau Wei Le, Bong Zhan Yong, Mohd Fauzi Yaakub;* ***analysis and interpretation of results:*** *Lau Wei Le, Bong Zhan Yong;* ***draft manuscript preparation:*** *Mohd Fadhli Zulkafli, Lau Wei Le, Bong Zhan Yong, Syafiqah Nur Azrie Safri. All authors reviewed the results and approved the final version of the manuscript.*

References

[1] Ankur Utsav, Amit Abhishek, P. Suraj & Ritesh Kr. Badhai (2021) An IoT Based UAV Network For Military Applications, in: 2021 Sixth International Conference on Wireless Communications, Signal Processing and Networking (WiSPNET), IEEE, 122–125. https://doi.org/10.1109/WiSPNET51692.2021.9419470

[2] Sudhir Kumar Chaturvedi, Raj Sekhar, Saikat Banerjee & Hutanshu Kamal (2019) Comparative Review Study of Military and Civilian Unmanned Aerial Vehicles (UAVs), *INCAS BULLETIN*, 11, 183–198. https://doi.org/10.13111/2066-8201.2019.11.3.16

[3] Zhu Xiaoning (2020) Analysis of military application of UAV swarm technology, in: 2020 3rd International Conference on Unmanned Systems (ICUS), IEEE, 1200–1204. https://doi.org/10.1109/ICUS50048.2020.9274974

[4] Arnau Rovira-Sugranes, Abolfazl Razi, Fatemeh Afghah & Jacob Chakareski (2022) A review of AI-enabled routing protocols for UAV networks: Trends, challenges, and future outlook, *Ad Hoc Networks*, 130, 102790. https://doi.org/10.1016/j.adhoc.2022.102790

[5] Panagiotis Radoglou-Grammatikis, Panagiotis Sarigiannidis, Thomas Lagkas & Ioannis Moscholios (2020), A compilation of UAV applications for precision agriculture, *Computer Networks*, 172, 107148. https://doi.org/10.1016/j.comnet.2020.107148

[6] Tsouros, Dimosthenis C., Stamatia Bibi, & Panagiotis G. Sarigiannidis (2019) A Review on UAV-Based Applications for Precision Agriculture, *Information*, 10, 349. https://doi.org/10.3390/info10110349

[7] Rafal Perz & Kacper Wronowski (2019) UAV application for precision agriculture, *Aircraft Engineering and Aerospace Technology*, 91, 257–263. https://doi.org/10.1108/AEAT-01-2018-0056

[8] J. Scherer & B. Rinner (2016) Persistent multi-UAV surveillance with energy and communication constraints, in: 2016 IEEE International Conference on Automation Science and Engineering (CASE), IEEE, 1225–1230. https://doi.org/10.1109/COASE.2016.7743546

[9] N.H. Motlagh, M. Bagaa & T. Taleb (2017) UAV-Based IoT Platform: A Crowd Surveillance Use Case, *IEEE Communications Magazine*, 55, 128–134. https://doi.org/10.1109/MCOM.2017.1600587CM

[10] F. Noor, M.A. Khan, A. Al-Zahrani, I. Ullah & K.A. Al-Dhlan (2020) A Review on Communications Perspective of Flying Ad-Hoc Networks: Key Enabling Wireless Technologies, Applications, Challenges and Open Research Topics, *Drones*, 4, 65. https://doi.org/10.3390/drones4040065

[11] *N.T. Hegde, V.I. George, C.G. Nayak & K. Kumar* (2019) Design, dynamic modelling and control of tilt-rotor UAVs: a review, *International Journal of Intelligent Unmanned Systems*, 8, 143–161. https://doi.org/10.1108/IJIUS-01-2019-0001

[12] H. Lee & H.J. Kim (2017) Trajectory tracking control of multirotors from modelling to experiments: A survey, *International Journal of Control, Automation, and Systems*, 15, 81–292. https://doi.org/10.1007/s12555-015-0289-3

[13] C. Silva, W.R. Johnson, E. Solis, M.D. Patterson & K.R. Antcliff (2018) VTOL Urban Air Mobility Concept Vehicles for Technology Development, in: 2018 Aviation Technology, Integration, and Operations Conference, American Institute of Aeronautics and Astronautics, Reston, Virginia. https://doi.org/10.2514/6.2018-3847

[14] A. Misra, S. Jayachandran, S. Kenche, A. Katoch, A. Suresh, E. Gundabattini, S.K. Selvaraj & A.A. Legesse (2022) A Review on Vertical Take-Off and Landing (VTOL) Tilt-Rotor and Tilt Wing Unmanned Aerial Vehicles (UAVs), *Journal of Engineering*, 2022, 1–27. https://doi.org/10.1155/2022/1803638

[15] Y. Zhou, H. Zhao & Y. Liu (2020) An evaluative review of the VTOL technologies for unmanned and manned aerial vehicles, *Computer Communications*, 149, 356–369. https://doi.org/10.1016/j.comcom.2019.10.016

[16] A.S. Saeed, A.B. Younes, C. Cai & G. Cai (2018) A survey of hybrid Unmanned Aerial Vehicles, *Progress in Aerospace Sciences*, 98, 91–105. https://doi.org/10.1016/j.paerosci.2018.03.007

[17] A.S. Saeed, A.B. Younes, S. Islam, J. Dias, L. Seneviratne & G. Cai (2015) A review on the platform design, dynamic modeling and control of hybrid UAVs, in: 2015 International Conference on Unmanned Aircraft Systems (ICUAS), IEEE, 806–815. https://doi.org/10.1109/ICUAS.2015.7152365

[18] Z. Li & P. Xia (2017),Aeroelastic stability of full-span tiltrotor aircraft model in forward flight, *Chinese Journal of Aeronautics*, 30, 1885–1894. https://doi.org/10.1016/j.cja.2017.09.007

[19] L. Bauersfeld, L. Spannagl, G. Ducard & C. Onder (2021) MPC Flight Control for a Tilt-Rotor VTOL Aircraft, *IEEE Transactions on Aerospace Electronic System*, 57, 2395–2409. https://doi.org/10.1109/TAES.2021.3061819

[20] Mini Skywalker 840mm ARF, (n.d.). https://hobbyking.com/en_us/mini-skywalker-840mm-arf.html?srsltid=AfmBOorXlYcfBREscfnvsUsVxkscGUeA0BmRzmy5vcZ5TrcI9pwao4xS (accessed December 4, 2024).

[21] W. Saengphet & C. Thumthae (2016) Conceptual design of fixed wing-VTOL UAV for AED transport, in: The 7 Th TSME International Conference on Mechanical Engineering.

[22] N.A. Vu, D.K. Dang & T. Le Dinh (2019) Electric propulsion system sizing methodology for an agriculture multicopter, *Aerospace Science Technology*, 90, 314–326. https://doi.org/10.1016/j.ast.2019.04.044

[23] V. Etacheri, R. Marom, R. Elazari, G. Salitra & D. Aurbach (2011) Challenges in the development of advanced Li-ion batteries: a review, *Energy Environmental Science*, 4, 3243. https://doi.org/10.1039/c1ee01598b

[24] S. Panigrahi, Y.S.S. Krishna & A. Thondiyath (2021) Design, Analysis, and Testing of a Hybrid VTOL Tilt-Rotor UAV for Increased Endurance, *Sensors*, 21, 5987. https://doi.org/10.3390/s21185987

[25] B.L. Bramfitt (2005) Carbon and Alloy Steels, in: Mechanical Engineers' Handbook, *Wiley*, 1–38. https://doi.org/10.1002/0471777447.ch1

[26] E.J. Pavlina & C.J. Van Tyne (2008) Correlation of Yield Strength and Tensile Strength with Hardness for Steels, *Journal of Materials Engineering and Performance*, 17, 888–893. https://doi.org/10.1007/s11665-008-9225-5

[27] D.J. Oehlers & R. Seracino (2004) Flexural Strength and Ductility, in: Design of FRP and Steel Plated RC Structures, *Elsevier*, 46–99. https://doi.org/10.1016/B978-008044548-9/50004-5